Werk

Terms and Conditions

Contact

Niedersächsische Staats- und Universitätsbibliothek Göttingen
Georg-August-Universität Göttingen
Platz der Göttinger Sieben 1
37073 Göttingen
Germany
Email: gdz@sub.uni-goettingen.de

J. Geophys. 42, 361 – 372, 1977

Journal of Geophysics

The Diurnal Variation of the Electron Density of the Mid-Latitude Ionospheric D-Region Deduced from VLF-Measurements

J. Schäfer

Astronomical Institutes, University of Bonn, Auf dem Hügel 71, D-5300 Bonn, Federal Republic of Germany

Abstract. Amplitude and phase of the components of the electric and magnetic field of the VLF-transmitter GBR (16 kHz, near Rugby/England) observed at the 3 receiving stations Stockert (near Bonn), Braunschweig and Berlin have been related to the electron density profile of the ionospheric D-layer via an appropriate propagation theory. The calculated wave parameters have been plotted as contour lines in a map containing as coordinates a characteristic height and the number of the electron density at this height. From that the diurnal variations of the electron density profile during summer and winter as well as the behaviour of the D-region during solar flare events have been deduced.

Key words: VLF-propagation – Electron density profile of the ionospheric D-layer – Diurnal variations of VLF field quantities.

1. Introduction

VLF-waves (3–30 kHz) can propagate within the atmospheric wave guide between the surface and the ionospheric D-layer. While the earth's surface behaves like a sharp boundary for these waves, the ionospheric D-layer is an inhomogeneous and anisotropic reflector for VLF-waves. Any variation of the electron density profile changes the reflection coefficient of the VLF-waves in amplitude and phase. Therefore the measurement of the electric and the magnetic field vectors of a commercial VLF-transmitter enables one to deduce this variation of the ionospheric electrons density via an appropriate theory.

For propagation paths up to about 1500 km, ray optics is a reasonable approximation for VLF-propagation (Volland, 1968). In this case the theoretical interpretation of the observed field parameters must be done in 2 steps. Firstly, one has to calculate the reflection matrix of an anisotropic, homogeneously layered ionosphere with respect to plane waves, and a virtual reflection height has to be defined. Secondly the elements of the reflection matrix and the virtual

height as function of the angle of incidence, of the geomagnetic field and of the electron density and collision frequency profile are used to determine the vectors of the electric and the magnetic field strength from ray optics theory. Summaries of the theoretical foundation of the reflection matrix and of the VLF-propagation theory have been given by Budden (1961), Wait (1962), Volland (1968) and Galejs (1972).

Using Budden's formulation, a Runge-Kutta-integration procedure for numerical calculation of the ionospheric reflection matrix has been described by Pitteway (1965). More convenient and appropriate for computer calculation is the matricant algorithm developed by Volland (1968). This simple procedure has been used in the following calculations.

Measurements of the field of VLF-transmitters have been analysed e.g. by Bracewell et al. (1951), Volland (1968), Frisius (1970) and Stratmann (1970), for only one field component. Model fitting with discrete D-layer models for VLF propagation over great distances has been carried out by Rinnert (1972) using mode theory. In the present paper model calculations via ray optics have been adjusted to measurements of the complete electromagnetic field of the transmitter GBR recorded at 3 receiving stations. The use of a fast computer and an appropriate calculation algorithm made it possible to determine amplitude and phase of all components of the electromagnetic field for a large number of ionospheric models. The results are presented as contour mappings for each component. This method allows one to determine directly the variation of field quantities as a function of the parameters of the ionospheric D-layer model.

2. The Calculation of the Reflection Matrix

The reflection coefficient of the plane earth with respect to plane waves of frequency ω, incident at angle θ, is given by the Fresnel formulas:

$$R_{\mathrm{TM}} = \frac{n_E^2 \cos \Theta - (n_E^2 - \sin^2 \Theta)^{0.5}}{n_E^2 \cos \Theta + (n_E^2 - \sin^2 \Theta)^{0.5}}, \text{ for TM-waves} \tag{1}$$

$$R_{\mathrm{TE}} = \frac{\cos \Theta - (n_E^2 - \sin^2 \Theta)^{0.5}}{\cos \Theta + (n_E^2 - \sin^2 \Theta)^{0.5}}, \text{ for TE-waves} \tag{2}$$

with the refraction-index of the earth:

$$n_E = \left(\varepsilon_E - \frac{i \sigma_E}{\omega \varepsilon_0}\right)^{0.5}. \tag{3}$$

The electric conductivity σ_E varies between $4\,\Omega^{-1}\,\mathrm{m}^{-1}$ for seawater and $10^{-4}\,\Omega^{-1}\,\mathrm{m}^{-1}$ for dry ground, and the dielectric constant ε_E is between 80 and 1 for these 2 cases. ε_0 is the dielectric constant of vacuum.

To determine the reflection properties of the ionosphere, the D-region is divided into horizontal homogeneous slabs of appropriate thickness. If the propagation plane of a homogeneous plane wave is in the $x-z$-plane of a cartesian system with z vertically upward, Maxwell's equations can be written in the form:

$$\mathbf{c}' = -i k_0 \mathbf{K}\,\mathbf{c} \tag{4}$$

with the field strength vector:

$$\mathbf{c}=\frac{1}{\sqrt{Z_0}}\begin{pmatrix} E_x \\ Z_0 H_x \\ Z_0 H_y \\ -E_y \end{pmatrix}, \qquad \mathbf{c}'=\frac{\partial c}{\partial z} \tag{5}$$

and **K**, a complex 4×4 coefficient matrix (Volland, 1968). Z_0 is the characteristic impedance of free space and k_0 is the wave number in vacuum. The matrix **K** is a function of the electron-neutral collision number, the geomagnetic field and of the electron density profile. Integration between the upper and lower boundary of a slab, z_2 and z_1, yields:

$$\mathbf{c}(z_1)=\mathbf{T}\,\mathbf{c}(z_2), \tag{6}$$

with T a transmission matrix, which is called "matrizant":

$$\mathbf{T}=\exp(i k_0 \mathbf{K}\cdot(z_2-z_1)). \tag{7}$$

If an appropriate linear-combination of field quantities is used,

$$\mathbf{a}=\mathbf{Q}^{-1}\mathbf{c}, \qquad \mathbf{a}=\begin{pmatrix} A_1 \\ A_2 \\ B_1 \\ B_2 \end{pmatrix}, \tag{8}$$

the coefficient matrix becomes diagonal:

$$\mathbf{a}'=-i k_0 \mathbf{N}\,\mathbf{a}. \tag{9}$$

The components of the vector **a** are two upgoing characteristic waves A_1 and A_2 and 2 downgoing characteristic waves B_1 and B_2. In vacuum A_1 and B_1 are pure TM-waves and A_2 and B_2 are pure TE-waves. The transmission behaviour of a slab with respect to characteristic waves is given by a matrix **M**:

$$\mathbf{a}(z_1)=\mathbf{M}\,\mathbf{a}(z_2), \qquad \mathbf{M}=\mathbf{Q}^{-1}T\,\mathbf{Q}. \tag{10}$$

Defining the reflection-matrix of a homogeneous layered ionosphere by:

$$\mathbf{R}\begin{pmatrix} A_1 \\ A_2 \end{pmatrix}=\begin{pmatrix} R_{\mathrm{TMTM}} & R_{\mathrm{TMTE}} \\ R_{\mathrm{TETM}} & R_{\mathrm{TETE}} \end{pmatrix}\cdot\begin{pmatrix} A_1 \\ A_2 \end{pmatrix}=\begin{pmatrix} B_1 \\ B_2 \end{pmatrix}, \tag{11}$$

one obtains from Equation 9 and after elimination of A_1 and A_2:

$$\mathbf{R}(z_1)=(\mathbf{M}_3+\mathbf{M}_4\,\mathbf{R}(z_2))\,(\mathbf{M}_1+\mathbf{M}_2\,R(z_2))^{-1}, \tag{12}$$

where $\mathbf{M}_i$ are the submatrices (2×2) of **M**. Thus one can determine the reflection-matrix of the whole ionosphere by repeatedly adding homogeneous slabs for any ionospheric model, angel of incidence or geomagnetic field (Frisius and Schäfer, 1976).

3. The Ray Optics Theory

The EM-field at the receiver represents the superposition of waves propagating along various ray paths. The waves, which are reflected at least once at the iono-

sphere, depend on the radiation characteristics of the transmitter as well as on the reflection properties of the earth and ionosphere. Sommerfeld's (1947) theory is applicable for the ground-wave. A superposition of all ionospheric waves and the ground wave yields the field of a vertical dipole (in cylindrical coordinates):

$$\begin{pmatrix} E_\rho \\ Z_0 H_\rho \end{pmatrix} = C \cdot \left(2\mathbf{W}(\rho)/n_E + \sum_{n=1}^{\infty} \{(\mathbf{R}_i \mathbf{R}_e)^n (\mathbf{I} + \mathbf{R}_e^{-1}) - (\mathbf{R}_e \mathbf{R}_i)^n (\mathbf{I} + \mathbf{R}_e)\} \sin^2 \theta_n \right.$$
$$\left. \cos \theta_n \exp(i k_0 (\rho - r_n)) \right) \cdot \begin{pmatrix} p_e \\ p_m \end{pmatrix}$$

$$\begin{pmatrix} E_z \\ Z_0 H_z \end{pmatrix} = C \cdot \left(2\mathbf{W}(\rho) + \sum_{n=1}^{\infty} \{(\mathbf{R}_i \mathbf{R}_e)^n (\mathbf{I} + \mathbf{R}_e^{-1}) + (\mathbf{R}_e \mathbf{R}_i)^n (\mathbf{I} + \mathbf{R}_e)\} \sin^3 \theta_n \right.$$
$$\left. \exp(i k_0 (\rho - r_n)) \right) \cdot \begin{pmatrix} p_e \\ p_m \end{pmatrix}$$

$$\begin{pmatrix} Z_0 H_\phi \\ -E_\phi \end{pmatrix} = -C \cdot \left(2\mathbf{W}(\rho) + \sum_{n=1}^{\infty} \{(\mathbf{R}_i \mathbf{R}_e)^n (\mathbf{I} + \mathbf{R}_e^{-1}) + (\mathbf{R}_e \mathbf{R}_i)^n (\mathbf{I} + \mathbf{R}_e)\} \sin^2 \theta_n \right.$$
$$\left. \exp(i k_0 (\rho - r_n)) \right) \cdot \begin{pmatrix} p_e \\ p_m \end{pmatrix} \tag{13}$$

where $\mathbf{R}_e$ and $\mathbf{R}_i$ are the reflection matrices of earth and ionosphere, p_e and p_m are the electric and magnetic dipole moments of the transmitter, $\mathbf{I}$ is the unit matrix, $\mathbf{W}(\rho)$ is the ground wave and

$$C = \frac{\omega Z_0 k_0 \exp(-i k_0 \rho)}{4\pi \rho},$$

is the field of a vertical dipole in free space. ρ is the distance transmitter-receiver and r_n the length of the ray path of a reflection order n.

A VLF-transmitter can be modelled sufficiently well by a vertical electric dipole ($p_m = 0$), for which in free space only the components E_z, E_ρ, H_ϕ exist. The conversion factors (non-diagonal members in $\mathbf{R}_i$) will, however, cause the appearence of additional field components H_ρ, H_z, E_ϕ for VLF-propagation in the terrestrial wave guide.

The values of the angles of incidence θ_n and of the ray paths r_n must be determined by taking into account the earth's curvature and the reflection heights for each reflection order. Neglecting or approximating these quantities would cause a considerable displacement of the interference pattern of ionospheric and ground waves. In addition, a convergence factor has to be introduced into the field strength calculation, which accounts for the focussing or defocussing of the wave energy density because of the curved reflectors (Bremmer, 1949).

4. The Data

Measurements for this analysis were available from Stockert near Bonn (distance GBR-Stockert: 580 km), Braunschweig (790 km) and Berlin (980 km). Amplitude and phase of the component H_ϕ of the transmitter GBR have been recorded since 1967 at the Stockert station. The phase measurements are stabilized by a

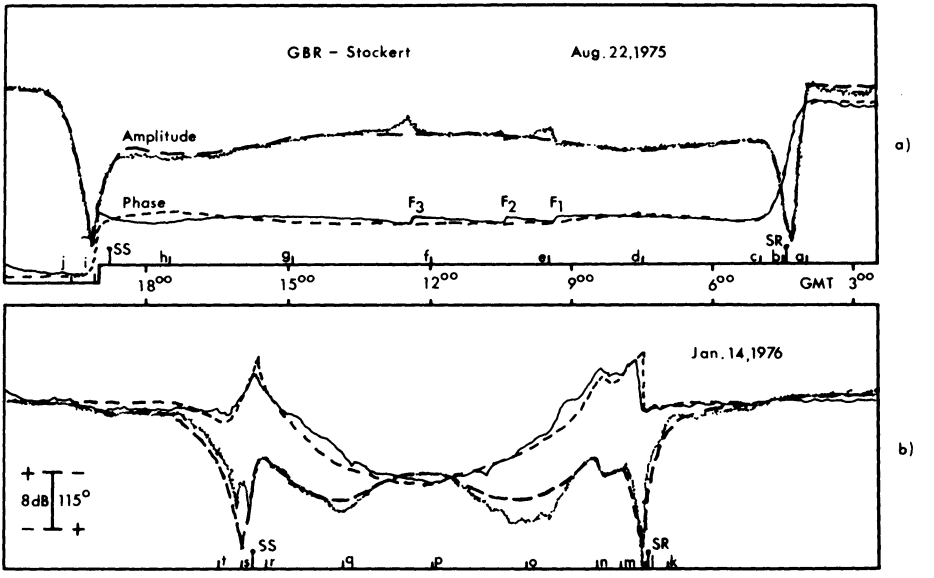

Fig. 1. Typical examples of the diurnal variations of amplitude and phase of the component H_ϕ at summer- and wintertime for the propagation path GBR-Stockert. The broken curves result from the fitting process. The time marks correspond to those in Figure 3. Solar flare events are indicated by "F"

rubidium frequency standard. Differences of 0.2 dB in amplitude and 4 deg in phase can be distinguished on the recordings. Examples of registrations are shown in Figure 1.

Another receiver, developed at the Heinrich-Hertz-Institute (HHI) in Berlin, measures the amplitudes of E_z and H_ϕ, the phase of E_z, the direction of arrival Φ, and the ratio of the smaller to the larger axis of the horizontal magnetic vector (HPR = H-polarisation-ratio) (Frisius et al., 1971). Similar detectors are operating at Braunschweig and Berlin. A monthly review of the results of all 3 stations has been published for the year 1971 by the HHI, Berlin. An example is shown in Figure 4.

5. The Graphical Presentation of the Field Quantities in a Contour Map

VFL-waves are reflected at heights where the electron density reaches a few hundreds of electrons cm^{-3}. Therefore the ionospheric D-layer is responsible for reflection of VFL-waves at daytime, while at night they are reflected at the E-layer.

Since the primary effects upon VLF-propagation arise from variations in the ionospheric electron density distribution (Rinnert, 1972), and since only relatively small variations of the collision frequency occur in the course of the day, it is reasonable to assume a collision frequency independent of time. The chosen dependence of collision frequency ν on the height z is (Frisius, 1974):

$$\nu(z) = 5 \times 10^6 \exp\left(\frac{70 - z}{6.7}\right) (s^{-1}), \tag{14}$$

which is valid at altitudes between about 60 and 110 km (Galejs, 1972).

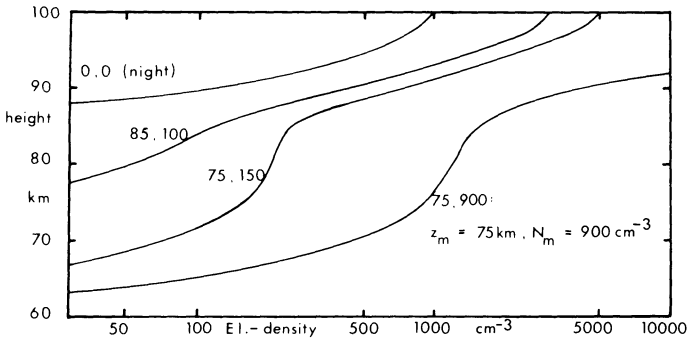

Fig. 2. Electron density profiles of the lower ionosphere with different parameters N_m and z_m of the D-layer

Within the ionospheric D-layer, where the effective recombination coefficient is proportional to

$$\exp\left(\frac{z_m - z}{H_s}\right),$$

Chapman theory leads to an electron density profile of the form:

$$N_e(z) = N_m \exp\left(0.5\left(1 - \exp\left(\frac{z_m - z}{H_s}\right)\right)\right), \tag{15}$$

where N_m is the density at a reference height z_m, and H_s is the scale height. Whereas VLF-waves are reflected at this layer during the day, the D-layer vanishes nearly completely at nighttime, and the VFL-waves are then reflected at the E-layer. For convenience, the same profile (Eq. (15)) has been used for this layer, with a constant reference height of $z_m = 100$ km and a density N_m, which is 30 times larger than the value of N_m of the D-layer, at least 1000 cm^{-3}, however. The exact profile of the electron density at heights where N_e exceeds 1000 cm^{-3} is not relevant for VLF-propagation, because the reflection occurs below these heights. A first comparison between theory and observations revealed, that the data could be best reproduced with a constant scale height value of $H_s = 6$ km within the D- and E-layers.

The remaining parameters are the variables N_m and z_m of the D-layer. Using fixed conditions for the propagation path, the magnetic field, the properties of the ground and the collision frequency, the amplitudes and phases of the EM-field components depend now only on these two parameters. By varying N_m and z_m over a wide range, a large number of D-layer models used in the literature and many of the observed electron density profiles can be well approximated. Some of these profiles with different values of N_m and z_m are plotted in Figure 2.

To obtain a graphical presentation, the field values of each propagation path have been calculated at more than 300 control points, i.e. for N_m in a range between 0 and 1200 cm^{-3} at intervals of 50 cm^{-3} and for z_m between 60 and 90 km at intervals of 2.5 km. By using a plotter contouring program, diagrams for the different components have been obtained (Figs. 3, 5 and 6). Amplitudes are given in dB relative to free space field strength, phases in degrees. This representation

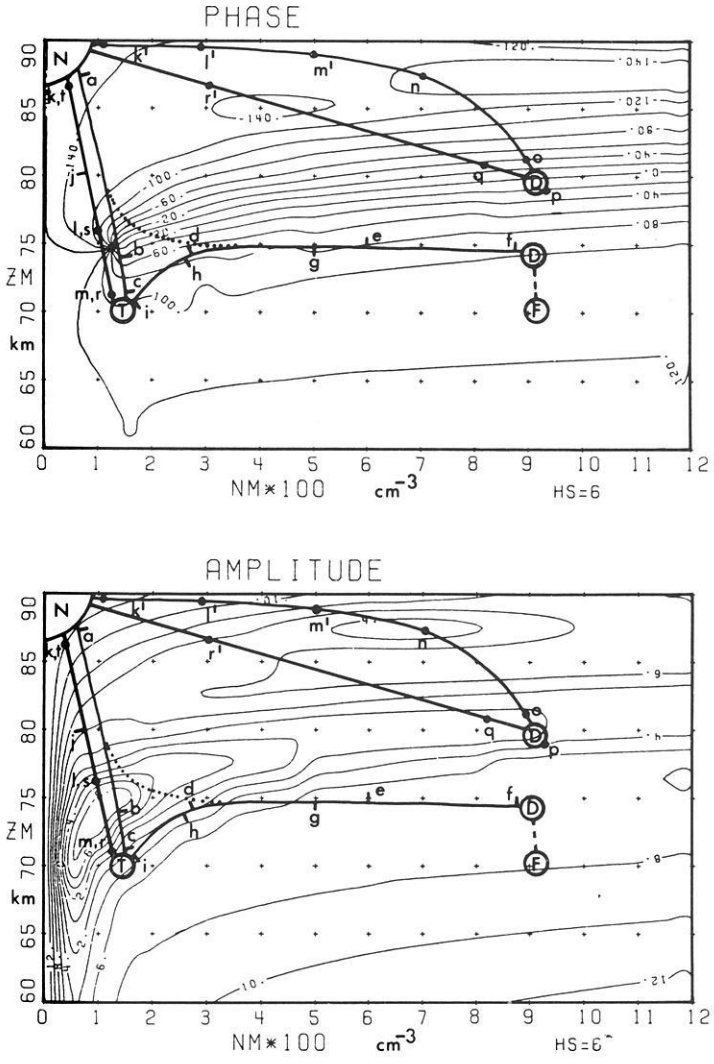

Fig. 3. Contour maps of phase and amplitude of H_ϕ for the propagation path GBR-Stockert. Amplitudes are given in dB relative to free space field strength, phases in degrees

allows, e.g., the simulation of a D-layer, in which the electron density parameter varies from $N_m = 0$ to $N_m = 1000\,\mathrm{cm}^{-3}$ at a constant height of $z_m = 60$ km. On the other hand a layer can be formed, which decreases its height parameter z_m from 90 km to 60 km at a constant electron content of $N_m = 1000\,\mathrm{cm}^{-3}$. One of these possibilities, or a mixture of them is taken at sunrise. A very special feature can be seen on the plot of H_ϕ for the propagation path GBR-Stockert (Fig. 3). Near the control point $N_m = 100\,\mathrm{cm}^{-3}$, $z_m = 75$ km the field strength vanishes completely, and all phase contour lines converge. For this model and for this propagation path the ionospheric waves and the ground wave are equal in magnitude but phase shifted by 180 deg. The destructive interference leads to zero field strength.

6. Fitting an Ionospheric Model

The fitting process shall be demonstrated here for the propagation example GBR-Stockert. An analysis of the Stockert registrations of several years yields 2 main types of phase and amplitude curves for H_ϕ. The first ones are applicable mainly at summertime, the second are appropriate only for winter. Two typical examples are shown in Figure 1.

The summer propagation type can be interpreted in the following manner: Before sunrise a nighttime E-layer exists together with a depleted D-layer beneath with parameters $N_m < 100\,\mathrm{cm}^{-3}$ and $z_m = 85$–$90\,\mathrm{km}$. In the $N_m - z_m$-diagrams this nighttime region is marked by an "N". From the records (Fig. 1 a) one finds, that the daytime amplitudes are about 7 dB lower than at night, and the phases are nearly 250° larger. The noontime region is thus characterized by a point close to $N_m = 900\,\mathrm{cm}^{-3}$, $z_m = 74\,\mathrm{km}$, and is marked by a "D". The deep field strength minimum at and shortly before sunrise is caused by a thin layer with electron density $N_m = 150\,\mathrm{cm}^{-3}$ descending down to $z_m = 70\,\mathrm{km}$ (marked by "T"). This transient layer can be explained by the influence of solar radiation at solar zenith angles of more than 90° prior to ground sunrise (Thomas and Harrison, 1970). The further developement of the D-layer is essentially due to the increase of N_m at an approximately constant height of $z_m = 75\,\mathrm{km}$ on a path marked by the heavy line in the contour plots. Time marks are placed in Figures 1 a and 3 to facilitate comparison between the measurements and computed values. The broken lines in Figure 1 a are the curves resulting from the path in the contour map of Figure 3. They are in good agreement with the original recordings. When N_m has attained a value of about $300\,\mathrm{cm}^{-3}$ near 75 km height, the contour lines pass nearly parallel to the N_m-axis. Therefore a further increase in N_m at the same height z_m has only minimal effect on D-layer reflection properties and VLF-propagation. The phase curve sometimes decreases at sunrise to the value of 100°. This effect evidently occurs when the pole near $N_m = 100\,\mathrm{cm}^{-3}$, $z_m = 75\,\mathrm{km}$ is not passed in a clockwise manner, but in a mathematically positive sense. The return to night conditions at sunset is generally somewhat above the morning path, as indicated by the dotted line in Figure 3. Occassionally, however, the pole is passed clockwise, as can be concluded from the record of 8 Aug. 1975. A very thin layer, slowly disappearing after ground sunset, may be responsible for this occurence.

Calculations for the other two stations also show satisfying agreement with measurements. For example, the records of Braunschweig of 30 Aug. 1971 are shown in Figure 4 and compared with the calculations in Figures 5 and 6. The field strength minimum occurs here about 1 h earlier than at Bonn, because the valley is approximately 10 km higher than at Bonn (Figs. 1 and 3) and the build up of the thin layer takes about this time. The daytime value of the amplitude is only little below night conditions, while the phase difference is 180° (Fig. 3). This can be simulated quite well by the calculations.

Figure 6, as well as similar plots for the other stations, shows that no substantial further information can be obtained by measuring the additional quantities HPR (the H-voltage-power-ratio) and Φ (the direction of arrival), because

only very small changes of the contour lines occur within a large vicinity centered on the point "D" (noontime value near $N_m = 900\ \mathrm{cm}^{-3}$, $z_m = 75$ km). On the other hand many small variations are possible in the twilight regions (Fig. 6). In addition, inhomogenities in the ionospheric layers at sunrise and sunset may be important, especially for HPR and Φ. These effects cannot be simulated well by our model. Nevertheless, the increase of the quantity HPR and the decrease of the angle Φ during twilight (Fig. 4) agrees with the corresponding model calculations (Fig. 6).

The diurnal variation of the field parameters during winter is quite different. On the Stockert records, at least 2 relative minima of the magnetic field strength can be seen shortly before and about 2 hours after sunrise in Figure 1 b of 10 Jan. 1976. The first minimum is the deepest and sharpest. The sunset records are similar, except that the two minima are generally not so sharp. The phase decreases by about 100° relative to the night value near sunrise and sunset. At noon the phase is only about 150° greater than during night. These registrations suggest, that at least two separate layers influence the VLF-propagation during winter. The first is a pre ground sunrise layer, similar to the summer transient layer, but with smaller thickness. The pole is therefore passed closely on the left side (marked by the symbols $k-l-m$ in Fig. 2), from which the deep minimum in amplitude and the phase jump of 100° arises. During the same time a second layer develops out of the nighttime E-layer (the path $k'-l'-m'$ in Fig. 2). When this layer has reached the height $z_m = 79$ km (path $n-o-p$), the reflection characteristics of the VLF-waves are dominated by that layer, which has now swallowed the thin transient layer. Therefore the phase gradually increases again by about 250°. The amplitude has to go through the deep and broad valley near $z_m = 80$ km during the build-up of the daytime layer. At noon it reaches a point near $N_m = 900\ \mathrm{cm}^{-3}$, $z_m = 79$ km. The way back to night conditions is indicated by the time marks $p-q-r-s-t$ in Figures 1 and 3. When the daytime layer has been depleted down to a point "r" near sunset, the remaining transient layer again plays a decisive role (marks $r-s-t$). Here again the calculation (dashed line in Fig. 1 b) fits the observations quite well. This consistency between observations and theory also exists for the other two stations.

A special application of this method is the simulation of solar flare effects on the lower ionosphere. Solar flare events are accompanied by phase jumps in the H_ϕ-component of up to 30° and an amplitude increase up to 5 dB, as can be seen on the record of 8 Aug. 1975 (marked by "F" in Fig. 1 a). From the contour map in Figure 3 one notices, that a daytime phase increase always indicates a downward movement of the D-layer height. However, the magnitude of the variations in field strength and phase depends strongly on the undisturbed conditions. The VLF-signal variation during solar flares generally becomes smaller for larger N_m and smaller z_m of the undisturbed daytime model. In particular, the quantities HPR and Φ are completely unsuitable for the detection of solar flares because they are not significantly influenced. The mean downward displacement of the height parameter z_m during 30 solar flares observed at Stockert during 1975 was 3–4 km. The maximum observed decrease in z_m over this data set was 8 km. The downward movement of the summer D-layer during an average solar flare is indicated by the mark "F" in Figure 3.

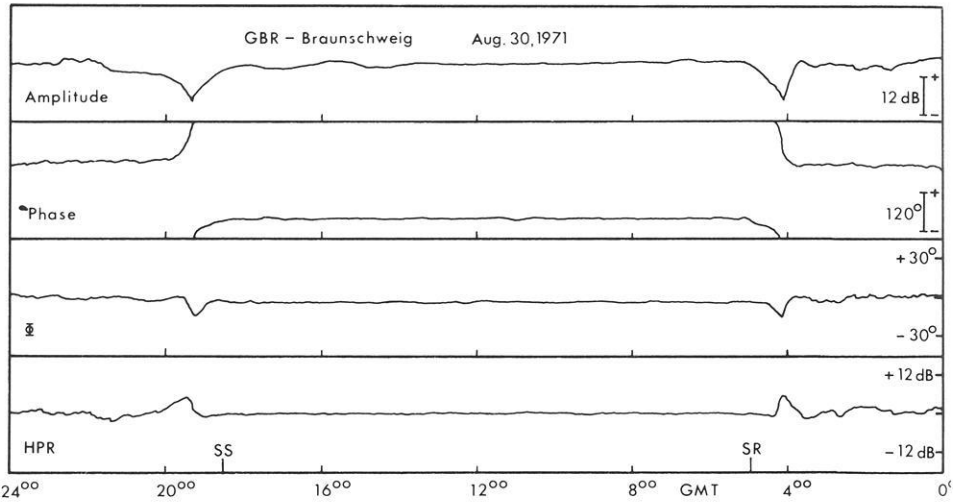

Fig. 4. Measurements of the VLF-signal of GBR at Braunschweig: Amplitudes of E_z and H_ϕ (coinciding), phase of E_z, angle of incidence Φ and H-polarisation-ratio HPR

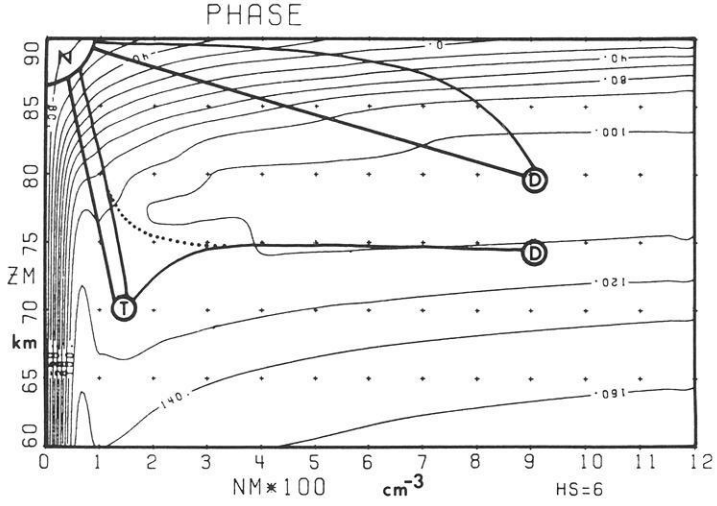

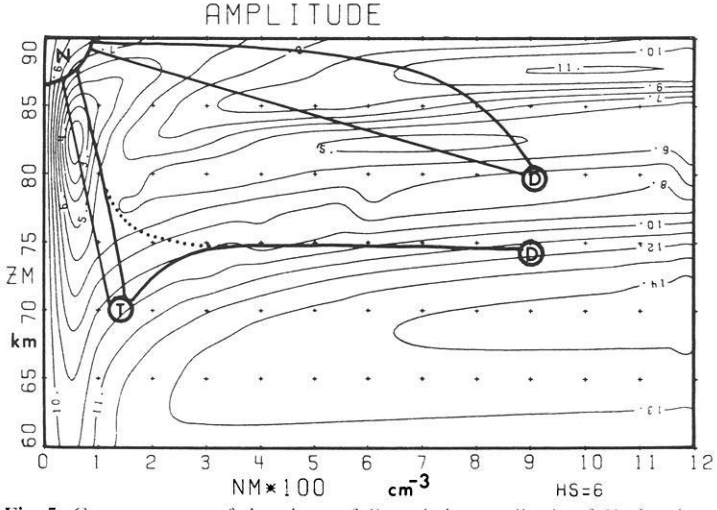

Fig. 5. Contour maps of the phase of E_z and the amplitude of H_ϕ for the propagation path GBR-Braunschweig

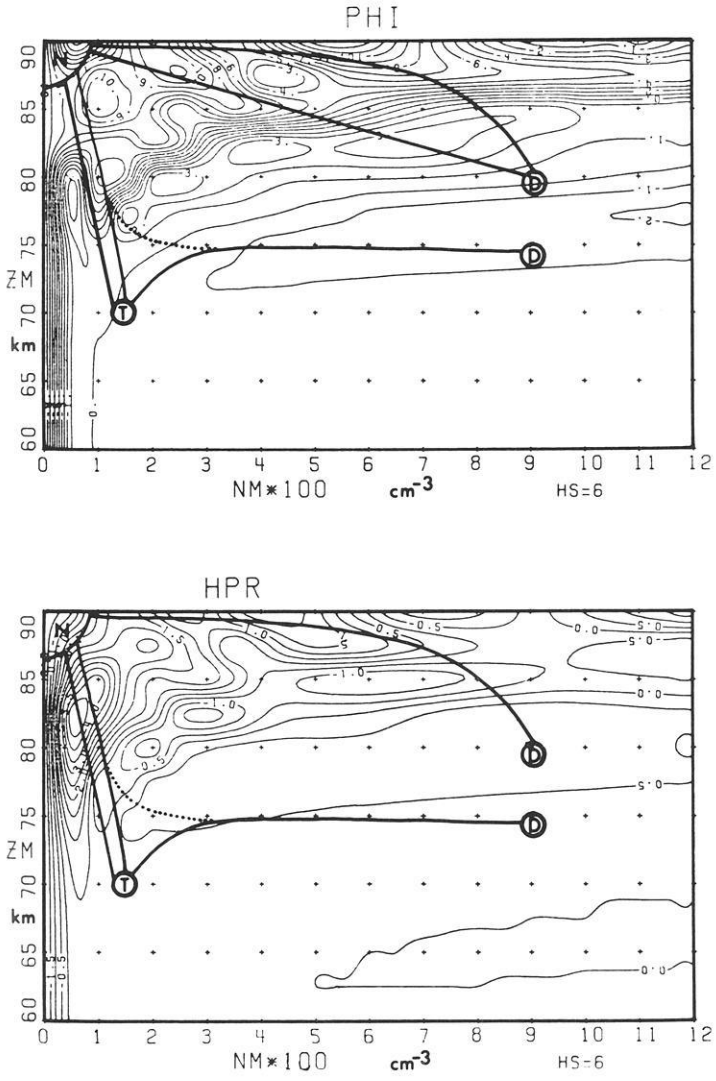

Fig. 6. Contour maps of HPR (in dB) and of the angle of incidence Φ (in degrees) for the propagation path GBR-Braunschweig

7. Conclusion

Contour maps for the components of the electromagnetic field of the VLF-transmitter GBR have been plotted using a full wave ray optics theory. The coordinates are the two parameters N_m and z_m, which characterize the electron density profile of the ionospheric D-layer: N_m is the electron content of the D-layer at a reference height z_m. From a comparison between theory and measurements the diurnal variations of the D-layer electron density as well as variations due to solar flares can be determined. The measurements of the transmitter GBR, made

at the receiving stations Stockert, Braunschweig and Berlin, indicate, that 2 general types of the diurnal D-layer variations occur. The first one, seen during summer months, can be simulated by the variation of the two parameters of a single layer. The second type occurs only during winter, when the lower boundary of the ionosphere is about 5 km higher than at summertime. The parameters of two independent layers have to be varied for a simulation of the diurnal behaviour of this model.

The occurence of a solar flare event causes a positive phase and amplitude shift in the H_ϕ-component of the Stockert records. One may deduce from the contour maps, that this behaviour is associated with a downward movement of the ionospheric D-layer over some kilometers.

Acknowledgement. I gratefully thank Prof. H. Volland for his encouragement and Dr. M. Bird for his critical reading and commenting on the first manuscript.

References

Bracewell, R. N., Budden, K. G., Radcliffe, S. A., Straker, T. W., Bremmer, H.: Terrestrial radio waves. Amsterdam: Elsevier

Budden, K. G.: Radio waves in the ionosphere. Cambridge: University Press 1961

Frisius, J.: Observations of diurnal amplitude and phase variations on 16 kHz transmission path and interpretation by a simple propagation model. AGARD Conference Proceedings, No. 33, K. Davies, ed. Slough, Engl.: Technivision Services 1970

Frisius, J.: Bemerkungen zur aeronomischen Interpretation von VLF-Registrierungen. Kleinheubacher Berichte **17**, 403, 1974

Frisius, J., Heydt, G., Raupach, R.: Measurement of the complete electromagnetic field of VLF transmitters. Techn. Bericht Nr. 145, HHI, Berlin 1971

Frisius, J., Schäfer, J.: Berechnung numerischer Näherungsfunktionen für die Reflexions- und Konversionsfaktoren der unteren Ionosphäre im Längstwellenbereich. Kleinheubacher Berichte, **19**, 517, 1976

Galejs, J.: Terrestrial propagation of long electromagnetic waves. Oxford: Pergamon Press 1972

HHI: Monthly reviews on VLF-CW-field strength measurements, Arbeitsgruppe VLF-Ausbreitung Heinrich-Hertz-Institut f. Schwingungsforschung, Berlin-Charlottenburg, 1971

Pitteway, M. L. V.: The numerical calculations of wave fields, reflection coefficient and polarisation for long radio waves in the lower ionosphere, Phil. Trans. Roy. Soc. London, Ser. A **257**, 219, 1965

Rinnert, K.: Untersuchungen der unteren Ionosphäre mit Hilfe der Längst-Wellenausbreitung über großen Entfernungen. Z. Geophys. **38**, 719, 1972

Sommerfeld, A.: 1947 Partielle Differentialgleichungen der Physik, 6. Aufl. Leipzig: Akad. Verlagsges. Geest u. Portig 1966

Stratmann, D.: Berechnung des Wellenfeldes eines Längstwellensenders im Entfernungsbereich bis 1000 km zur kontinuierlichen Sondierung der tiefen Ionosphäre durch Feldstärkenmessungen vom Sender. Mitteilungen aus dem MPI für Aeronomie. Berlin-Heidelberg-New York: Springer 1970

Thomas, L., Harrison, M. D.: The electron density distribution in the D-region during the night and pre sunrise period, J. Atmospheric. Terrest. Phys. **32**, 1, 1970

Volland, H.: Die Ausbreitung langer Wellen. Braunschweig: Vieweg 1968

Wait, J. R.: Electromagnetic waves in stratified media. London: Pergamon Press 1962

Weekes, K.: The ionospheric propagation of long and very long radio waves over distances less than 1000 km. Proc. IEE **98**, 221, 1951

Received August 11, 1976